

Low Loss and High Transmission Electromagnetically Induced Transparency (EIT) Effect in Cylindrical Through-Hole Dielectric Cubes

Lei Zhu^{1, 2}, Xin Zhao², Chun Hui Zhao^{1, *}, Liang Dong^{2, 3},
Feng Juan Miao², Chao Hui Wang⁴, and Jing Guo⁵

Abstract—We numerically demonstrate that an electromagnetically induced transparency (EIT) effect can be achieved in an all-dielectric metamaterial, whose micro unit consists of two cylindrical through-hole cubes (CTCs). Two CTCs produce electric and magnetic Mie resonances in the vicinity of 6.2 GHz, respectively. Specially, the appropriate control on the interaction between two Mie resonances can lead to destructive interference of scattering fields, and thus the EIT effect with low loss and high transmission can be achieved. The influences of key parameters of all-dielectric metamaterial on its EIT effects are also investigated. In addition, the slow wave property of proposed structure is verified by computing the group delay, and the superiority of CTC is discussed. Such an all-dielectric metamaterial may have potential applications in areas such as low loss slow wave devices and high sensitivity sensors.

1. INTRODUCTION

Electromagnetically induced transparency (EIT) is an important phenomenon in quantum optics, which is mainly caused by the quantum destructive interference between two different pathways [1]. It leads to a decreased absorption of light in the quantum system at its resonant frequency and produces a transparency window in the transmission spectrum [2]. In other words, an original opaque medium becomes transparent over a narrow spectrum [3]. When an EIT effect occurs, the dispersion property of system will also change significantly, resulting in characteristics such as the increase in refractive index, the decrease in group velocity of incident wave and the enhancement of nonlinear effect [3]. The realization of quantum EIT effect needs to meet special experimental conditions, but it is relatively easy to achieve the analog of EIT effect in metamaterials, plasmonic structures, coupled resonators, circuits and other systems [4–13]. Metamaterials are artificial composite materials that exhibit special electromagnetic properties based on periodic or aperiodic structures in sub-wavelength scale. In recent years, the EIT effect of metamaterial has attracted much attention due to its advantages of room temperature operability, large bandwidth, the ability to integrate with circuits, etc. [14].

Traditional metamaterials contain metallic materials that lead to high intrinsic losses inevitably. This limits the widespread application of metallic EIT metamaterials [15]. As a supplement and alternative, all-dielectric metamaterials have attracted the interest of many researchers in recent years. The micro units of all-dielectric metamaterials are made from high dielectric constant ceramics, silicon-based, graphene and other insulators or semiconductor mediums [16], which own the advantages of

Received 23 August 2018, Accepted 12 November 2018, Scheduled 13 December 2018

* Corresponding author: Chun Hui Zhao (zhaochunhui@hrbeu.edu.cn).

¹ College of Information and Communication Engineering, Harbin Engineering University, Harbin 150001, China. ² Communication and Electronics Engineering Institute, Qiqihar University, Qiqihar 161006, China. ³ School of Electronic Engineering, Beijing University of Posts and Telecommunications, Beijing 100876, China. ⁴ College of Materials Science and Technology, Qiqihar University, Qiqihar 161006, China. ⁵ Science and Technology on Electronic Test & Measurement Laboratory, Ministry of Education, North University of China, Taiyuan 030051, China.

low loss, wide band, simple structure, optical band extensibility, etc. [16]. The low loss displacement currents in all-dielectric metamaterials can also be used to replace the high loss ohmic currents in metallic metamaterials to provide the electric dipole, magnetic dipole, and higher order multistage resonances required by EIT effect [16].

There are two main methods to achieve EIT effect in metamaterials: One is to rely on near-field coupling between two resonators, and the other is to rely on the far-field coupling between two resonators (so-called phase coupling) [17, 18]. Generally, two common approaches are used for implementing EIT effects based on the near-field coupling. The first approach is to design two sub-structures in the micro unit of metamaterial. Two sub-structures work as bright and dark modes, respectively, where the bright mode is coupled directly with the incident wave, and the dark mode is indirectly excited by incident wave through near-field coupling with bright mode [14, 19–24]. This coupling between bright and dark modes produces an EIT effect. The second method is to design a superradiant (low Q -factor) resonator and a subradiant (high Q -factor) resonator in the micro unit of metamaterial, and both resonators can be directly excited by incident wave [20, 25]. In this case, the EIT effect can be achieved by appropriately adjusting the coupling between two resonators and thus causing the two resonators to generate electric and magnetic resonances around the same frequency, respectively [2, 15, 20, 26–28].

In this paper, the second method is adopted to realize EIT effect. Two kinds of cylindrical through-hole cubes (CTCs) are designed with the same dielectric constant and different sizes, and they are combined to form the micro unit of our metamaterial. We studied the EIT effect and its physical mechanism. Two CTCs produce electric and magnetic Mie resonances at around 6.2 GHz, respectively, and their interaction leads to destructive interference of scattering fields, thus the EIT effect is achieved. The influence of separation distance between two CTCs on the EIT effect is also discussed, and the slow wave performance of our metamaterial is investigated by calculating group delay. The simulation results indicate that the EIT effect is obtained in the vicinity of 6.2 GHz, and the group delay at transmission peak is about 2.79 ns. Moreover, the advantages of CTCs compared to solid cubes are discussed, and the simulation results show that our system has the superiorities of low loss and high transmission (transmittance of over 0.9). Such an all-dielectric EIT metamaterial may have potential applications in low loss slow waves and sensors, etc. [14–16, 29, 30].

2. STRUCTURE DESIGN AND SIMULATION

The micro unit of our metamaterial is shown in Figure 1. It consists of two cubes with cylindrical through-holes located in their geometric centers. The geometric centers of two cubes are placed along z -direction with a separation distance of s , and cylindrical through-holes are put along x -direction. The specific geometrical dimensions are designed as $d_1 = h_1 = 6.5$ mm, $r_1 = 1.5$ mm, $d_2 = h_2 = 5$ mm, $r_2 = 2$ mm, $s = 1$ mm, and $p_x = p_y = 12$ mm. The relative dielectric constant and loss tangent of dielectric cubes are set as $\epsilon_r = 110$ and $\delta = 0.0015$ [31]. In the simulation, we use periodic boundary condition. Plane electromagnetic wave propagates along z -direction with E -field and H -field along y -direction and x -direction, respectively.

Figure 2(a) shows the transmission spectrum of single small CTC. It can be seen that a transmission dip with a Q -factor about 394 occurs at 6.27 GHz. The transmission spectrum of single large CTC is

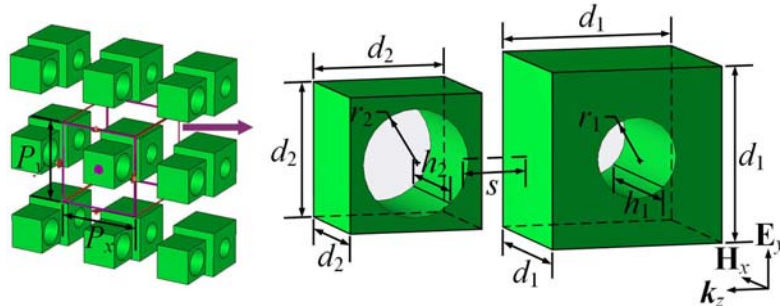


Figure 1. Micro unit of proposed structure and periodic array.

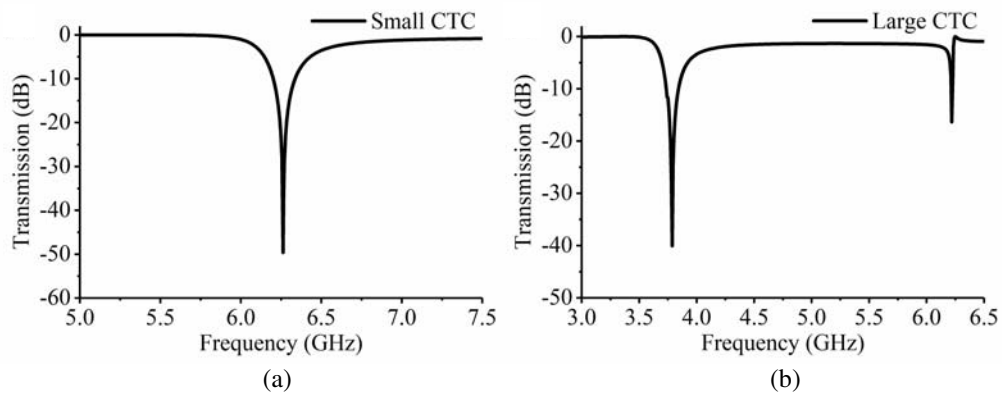


Figure 2. Simulated transmission spectra of single (a) small CTC and (b) large CTC.

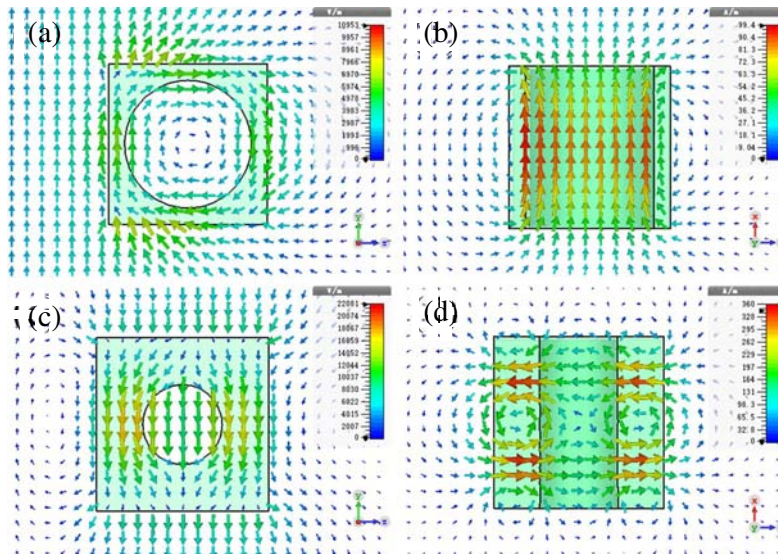


Figure 3. Simulated (a) *E*-field distribution and (b) *H*-field distribution of single small CTC (magnetic resonance) at 6.27 GHz, and simulated (c) *E*-field distribution and (d) *H*-field distribution of single large CTC (electric resonance) at 6.22 GHz.

displayed in Figure 2(b). It is indicated that the second transmission dip forms at 6.22 GHz with a *Q*-factor about 2244, which is sharper than that of small CTC. According to the all-dielectric Mie resonance theory [32], magnetic and electric dipole resonances will be excited when the frequency of incident wave is below or close to the bandgap frequency of a high index particle, making the particle behave as a magnetic dipole (first order Mie resonance) and an electric dipole (second order Mie resonance) [33]. Thus, the transmission dip of single small CTC in Figure 2(a) belongs to magnetic resonance, while the second transmission dip of single large CTC in Figure 2(b) belongs to electric resonance, which can be confirmed by the simulated field distributions, as shown in Figure 3.

As can be seen, a circular displacement current (see Figure 3(a)) and a symmetrical magnetic field (see Figure 3(b)) are formed in single small CTC at 6.27 GHz. They coincide with the unique circular displacement field and symmetrical magnetic field of magnetic Mie resonance [32, 33]. Therefore, the resonance of single small CTC belongs to the first order Mie resonance (magnetic resonance), and it corresponds to a magnetic dipole here. Similarly, for the resonance of single large CTC, the second transmission dip formed at 6.22 GHz has a symmetrical electric field (see Figure 3(c)), which belongs to an electric resonance (second order Mie resonance), and it is equivalent to an electric dipole here.

What should be pointed out is that due to the partition of through-hole, there are two loops instead of one loop in the magnetic field of single large CTC (see Figure 3(d)). But the two loops are interrelated to each other, and they are essentially a split of one loop.

It is obvious that these two resonances can be individually excited by coupling with incident wave, but their Q -factors differ by an order of magnitude. These characteristics are consistent with the second method of achieving EIT effect above. Thus, the small CTC operates as a superradiant element due to its wide resonant frequency band (low Q -factor) of magnetic resonance, while the large CTC works as a subradiant element because of its high Q -factor of electric resonance. When the two elements are combined as the structure in Figure 1, the interaction between them leads to destructive interference of scattering fields, and thus an evident EIT window is generated at around 6.2 GHz, as shown in Figure 4.

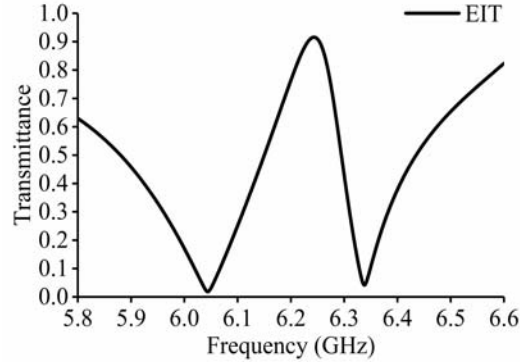


Figure 4. Simulated transmittance spectrum of proposed metamaterial.

In order to understand the physical mechanism of the EIT effect, we simulated the E -field and H -field distributions of EIT window at resonant frequencies. Figure 5 shows the corresponding E -field and H -field distributions of our structure. It can be seen that the electric resonance of large CTC and the magnetic resonance of small CTC occur concurrently. At the first transmission dip (6.04 GHz), the E -field of incident wave is mainly coupled with large CTC (see Figure 5(a)), and the H -fields in two CTCs are almost equal (see Figure 5(b)). On the two adjacent surfaces of two CTCs, there is an interaction between the scattering electromagnetic fields of CTCs. At the EIT center (see Figures 5(c)–(d)), due to the influences of E -field and H -field of large CTC, the shapes of E -field and H -field in small CTC are changed, and the coupling between two CTCs reaches the strongest. This destructive interference between scattering fields of two resonators makes the radiation loss of micro unit decrease significantly and thus results in an obvious transparency (transmission) window [28]. At this time, the E -field and H -field are concentrated inside the large CTC. However, when it comes to the second transmission dip (6.34 GHz), as shown in Figures 5(e)–(f), the E -field and H -field are distributed in both CTCs, and vast of the E -field is dissipated into free space, which means that the destructive interference disappears.

When the separation distance s between two CTCs is changed, the transmittance spectra and corresponding Q -factors of structure are shown in Figure 6. Here, we calculate the Q -factor as [18, 24, 26]

$$Q = f_0/\Delta f \quad (1)$$

where Δf denotes the full width at half maximum (FWHM) of EIT window, and f_0 represents the center frequency of EIT window. As shown in Figure 6(a), the EIT window narrows or even disappears with increase of s . Figure 6(b) shows that the Q -factor gets higher when s is increased. The reason for these variations is that different separation distances change the destructive interference strength between two CTCs. As the separation distance increases, the destructive interference strength becomes weaker, making the EIT effect sharper, and thus increasing the Q -factor. It should be noted that when $s = 1$ mm, the near-field coupling between two resonators becomes the strongest, resulting in the widest EIT window. In this case, Δf is around 0.16 GHz, and Q -factor is about 40.

The steep change in transmission phase within EIT transparent window results in a strong dispersion [34], which produces slow wave effect. The slow wave effect can be described by group

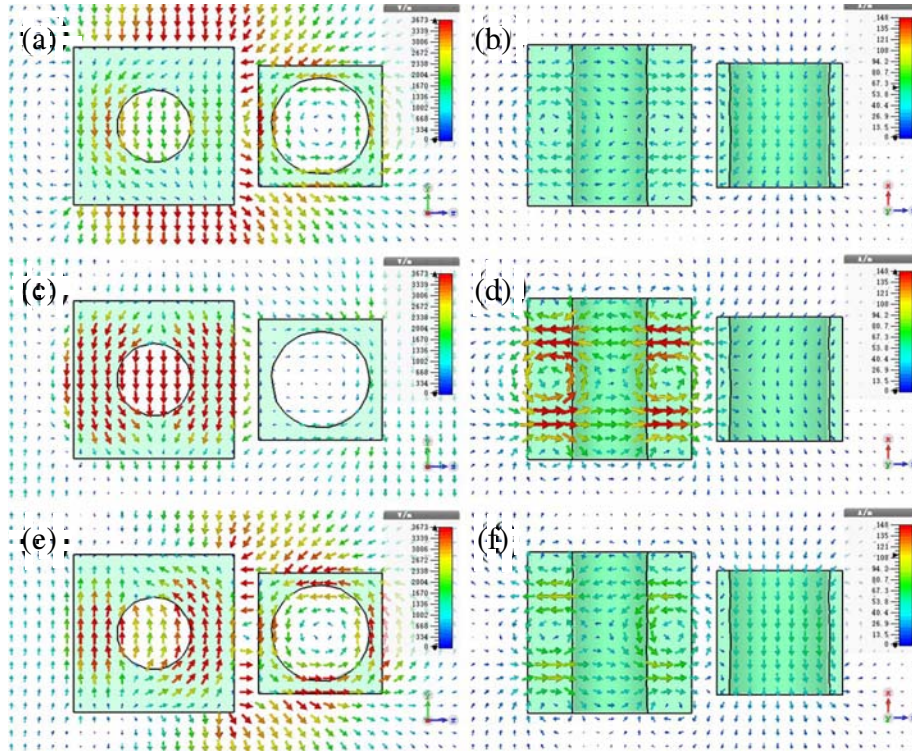


Figure 5. Simulated (a) E -field distribution (y - o - z plane) and (b) H -field distribution (x - o - z plane) at 6.04 GHz, (c) E -field distribution (y - o - z plane) and (d) H -field distribution (x - o - z plane) at 6.24 GHz, and (e) E -field distribution (y - o - z plane) and (f) H -field distribution (x - o - z plane) at 6.34 GHz.

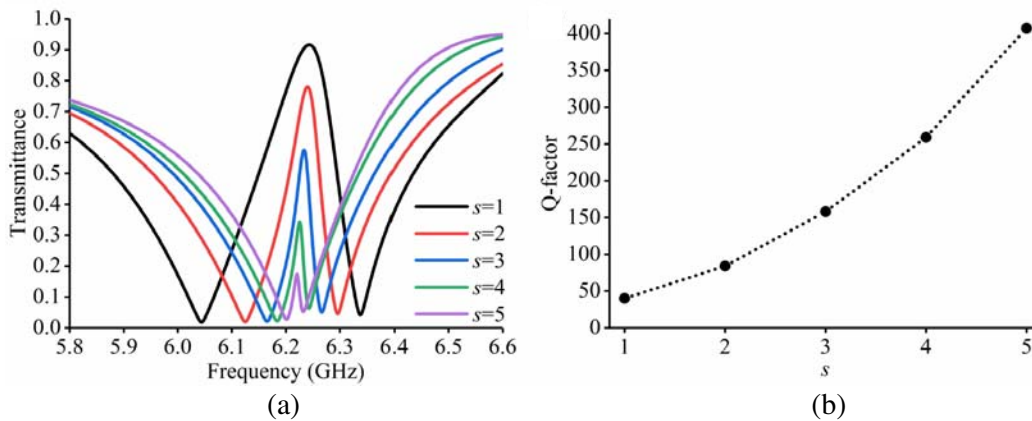


Figure 6. Simulated (a) transmittance spectra and (b) corresponding Q -factor of system with s changing from 1 to 5 mm.

delay [34]. Here, we estimate group delay by the following formula [34, 35]

$$\tau_g = -d\varphi/d\omega \tag{2}$$

where φ denotes the transmission phase, and $\omega = 2\pi f$ [35] represents the angular frequency. The simulated transmission phase and calculated group delay are plotted in Figure 7. The simulated transmission phase displayed in Figure 7(a) indicates that the phase changes drastically in the EIT window. Figure 7(b) shows that the group delay at transparent peak is about 2.79 ns, while the group delay through free space with the same thickness is about 0.04 ns (calculated by d/c_0 , where $d = 12.5$ mm

and c_0 is the speed of light in vacuum). The result numerically proves the slow wave property of proposed structure.

To better understand the role of holes, we contrast the EIT effect of proposed structure with that of solid cubes. When the CTCs in Figure 1 are replaced by two solid cubes with edge lengths of 5.2 mm and

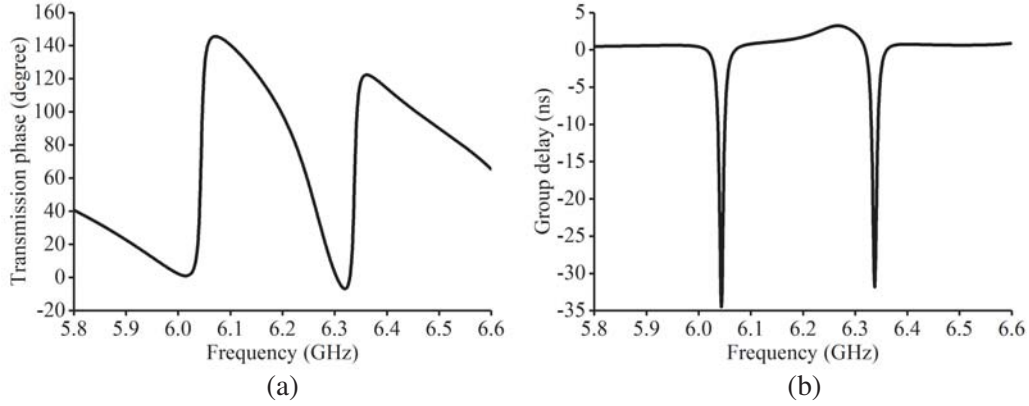


Figure 7. (a) Simulated transmission phase and (b) corresponding group delay.

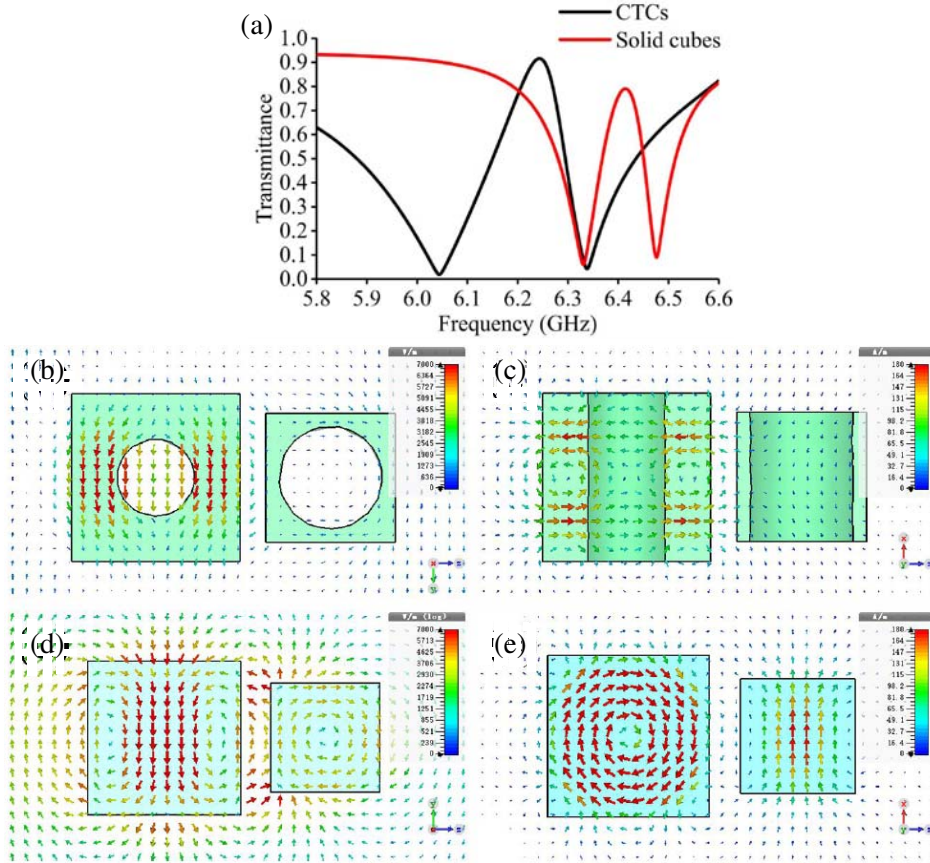


Figure 8. Simulated (a) transmittance spectra of CTCs and solid cubes structures, (b) E -field distribution (y - o - z plane) and (c) H -field distribution (x - o - z plane) of CTCs structure at its peak of EIT window, (d) E -field distribution (y - o - z plane) and (e) H -field distribution (x - o - z plane) of solid cubes structure at its peak of EIT window.

3.7 mm, there is still an EIT window at around 6.2 GHz, as shown in Figure 8(a) (red line). However, the new EIT window is smaller in peak, and its bandwidth is narrower. This is because the coupling between solid cubes is weaker, causing more E -field being lost into free space, as shown in Figures 8(b)–(e). In other words, for the same separation, the destructive interference between scattering fields of two solid cube resonators is weaker. This weaker destructive interference brings about higher radiation loss, thus results in a lower transmission peak. Therefore, the higher peak in the transparency window in Figure 8(a) results from lower (radiative) loss of the proposed structure compared with solid cubes. Besides, the peak resonant intensity of proposed structure within EIT window is larger than the values in references [11, 26, 27], which means that the loss for our structure is lower.

Generally, EIT effect in metamaterial results from the normal illumination [9–11, 20–28]. While the EIT resonance in our metamaterial is excited by the lateral illumination for EM waves. Although the thickness of our structure increases, we provide a new excitation method for achieving the EIT effect. Moreover, the lateral electrical size α ($\alpha = p/\lambda$, where p is the size of micro unit and λ the operating wavelength) of proposed structure (~ 0.25) is smaller than that in references [11, 21, 26, 27] (~ 0.28 , ~ 0.59 , ~ 0.50 and ~ 0.43), which means that our structure possesses better miniaturization in lateral size.

3. CONCLUSION

In summary, we have proposed an all-dielectric EIT metamaterial. Low loss and high transmission EIT effect has been obtained at around 6.2 GHz by using two cylindrical through-hole cubes with different dimensions. We have illustrated the exciting mechanism of EIT effect based on the superradiant and subradiant model. The influence of separation distance between two dielectric cubes on transmittance and Q -factor for transparency window has also been discussed. Results indicate that the coupling strength variation of destructive interference between superradiant and subradiant modes leads to different resonance characteristics for EIT window. Moreover, the slow wave property of our structure has also been verified by calculating the group delay. In addition, the superiority of through-hole cube in broadening bandwidth and reducing loss is demonstrated by our design. The metamaterial has advantages of less loss and higher transmittance (more than 0.9) than common metallic EIT metamaterials, which may be applied in domains such as low loss slow wave devices and high sensitivity sensors.

ACKNOWLEDGMENT

This work is supported by the National Natural Science Foundation of China (Grant Nos. 61501275, 61701141), the China Postdoctoral Science Special Foundation (Grant No. 2018T110274), the China postdoctoral science foundation (Grant No. 2017M611357), the Science Foundation Project of Heilongjiang Province of China (Grant No. QC2015073), the postdoctoral science foundation of Heilongjiang Province of China (Grant No. LBH-Z17045), the Young creative talents training plan of general universities of Heilongjiang Province of China (Grant No. UNPYSCT-2017152), and the technology bureau of Qiqihar city of Heilongjiang Province of China (Grant No. GYGG-201511).

REFERENCES

1. Harris, S. E., J. E. Field, and A. Imamoglu, "Nonlinear optical processes using electromagnetically induced transparency," *Physical Review Letters*, 1107–1110, Vol. 64, 1990.
2. Boller, K. J., A. Imamoglu, and S. E. Harris, "Observation of electromagnetically induced transparency," *Physical Review Letters*, Vol. 66, 2593–2596, 1991.
3. Fleischhauer, M., A. Imamoglu, and J. P. Marangos, "Electromagnetically induced transparency: Optics in coherent media," *Reviews of Modern Physics*, Vol. 77, 633–673, 2005.
4. Khardikov, V. V., E. O. Iarko, and S. L. Prosvirnin, "A giant red shift and enhancement of the light confinement in a planar array of dielectric bars," *J. Opt.*, Vol. 14, 035103, 2012.

5. Tidstrom, J., C. W. Neff, and L. M. Andersson, "Photonic crystal cavity embedded in electromagnetically induced transparency media," *J. Opt.*, Vol. 12, 035105, 2010.
6. Wan, M. L., J. N. He, Y. L. Song, and F. Q. Zhou, "Electromagnetically induced transparency and absorption in plasmonic metasurfaces based on near-field coupling," *Physics Letters A*, Vol. 379, 1791–1795, 2015.
7. Hu, S., H. L. Yang, S. Han, X. J. Huang, and B. X. Xiao, "Tailoring dual-band electromagnetically induced transparency in planar metamaterials," *J. Appl. Phys.*, Vol. 117, 043107, 2015.
8. Alonso-Gonzalez, P., P. Albella, F. Golmar, L. Arzubiaga, F. Casanova, L. E. Hueso, J. Aizpurua, and R. Hillenbrand, "Visualizing the near-field coupling and interference of bonding and anti-bonding modes in infrared dimer nanoantennas," *Optics Express*, Vol. 21, 1270–1280, 2013.
9. Zhang, K., C. Wang, L. Qin, R. W. Peng, D. H. Xu, X. Xiong, and M. Wang, "Dual-mode electromagnetically induced transparency and slow light in a terahertz metamaterial," *Optics Letters*, Vol. 39, 3539–3542, 2014.
10. Duan, X. Y., S. Q. Chen, H. F. Yang, H. Cheng, J. J. Li, W. W. Liu, C. Z. Gu, and J. G. Tian, "Polarization-insensitive and wide-angle plasmonically induced transparency by planar metamaterials," *Appl. Phys. Lett.*, Vol. 101, 143105, 2012.
11. Papasimakis, N., V. A. Fedotov, N. I. Zheludev, and S. L. Prosvirnin, "Metamaterial analog of electromagnetically induced transparency," *Phys. Rev. Lett.*, Vol. 101, 253903, 2008.
12. Luk'yanchuk, B., N. I. Zheludev, S. A. Maier, N. J. Halas, P. Nordlander, H. Giessen, and C. T. Chong, "The Fano resonance in plasmonic nanostructures and metamaterials," *Nature Materials*, Vol. 9, 707–715, 2010.
13. Tassin, P., L. Zhang, T. Koschny, E. N. Economou, and C. M. Soukoulis, "Low-loss metamaterials based on classical electromagnetically induced transparency," *Phys. Rev. Lett.*, Vol. 102, 063901, 2009.
14. Vafapour, Z. and H. Alaei, "Achieving a high Q -factor and tunable slow-light via classical electromagnetically induced transparency (CI-EIT) in metamaterials," *Plasmonics*, Vol. 12, 479–488, 2017.
15. Zhu, L., L. Dong, J. Guo, F. Y. Meng, and Q. Wu, "Tunable electromagnetically induced transparency in hybrid graphene/all-dielectric metamaterial," *Appl. Phys. A*, Vol. 123, 192, 2017.
16. Ding, P., J. N. He, J. Q. Wang, C. Z. Fan, and E. J. Liang, "Electromagnetically induced transparency in all-dielectric metamaterial-waveguide system," *Applied Optics*, Vol. 54, 3708–3714, 2015.
17. Kekatpure, R. D., E. S. Barnard, W. Cai, and M. L. Brongersma, "Phase-coupled plasmon-induced transparency," *Physical Review Letters*, Vol. 104, 243902, 2010.
18. Jin, X. R., Y. H. Lu, J. Park, H. Y. Zheng, F. Gao, Y. Lee, J. Y. Rhee, K. W. Kim, H. Cheong, and W. H. Jang, "Manipulation of electromagnetically-induced transparency in planar metamaterials based on phase coupling," *J. Appl. Phys.*, Vol. 111, 073101, 2012.
19. Zhu, L., F. Y. Meng, L. Dong, Q. Wu, B. J. Che, J. Gao, J. H. Fu, K. Zhang, and G. H. Yang, "Magnetic metamaterial analog of electromagnetically induced transparency and absorption," *Journal of Applied Physics*, Vol. 117, 17D146, 2015.
20. Ding, C. F., Y. T. Zhang, J. Q. Yao, C. L. Sun, D. G. Xu, and G. Z. Zhang, "Reflection-type electromagnetically induced transparency analogue in terahertz metamaterials," *Chin. Phys. B*, Vol. 23, 124203, 2014.
21. Yang, Y. M., I. I. Kravchenko, D. P. Briggs, and J. Valentine, "Dielectric metasurface analogue of electromagnetically induced transparency," *Nat. Commun.*, Vol. 5, 5753, 2014.
22. Zhang, F. L., Q. Zhao, J. Zhou, and S. X. Wang, "Polarization and incidence insensitive dielectric electromagnetically induced transparency metamaterial," *Optics Express*, Vol. 21, 19675–19680, 2013.
23. Meng, F. Y., Q. Wu, D. Erni, K. Wu, and J. Lee, "Polarization-Independent Metamaterial analog of electromagnetically induced transparency for a refractive-index-based sensor," *IEEE Transactions on Microwave Theory and Techniques*, Vol. 60, 3013–3022, 2012.

24. Zhang, J. F., W. Liu, X. D. Yuan, and S. Q. Qin, "Electromagnetically induced transparency-like optical responses in all-dielectric metamaterials," *J. Opt.*, Vol. 16, 125102, 2014.
25. Zhang, S., A. G. Dentcho, Y. Wang, M. Liu, and X. Zhang, "Plasmon-induced transparency in metamaterials," *Phys. Rev. Lett.*, Vol. 101, 047401, 2008.
26. Li, H. M., S. B. Liu, S. Y. Liu, and H. F. Zhang, "Electromagnetically induced transparency with large group index induced by simultaneously exciting the electric and the magnetic resonance," *Appl. Phys. Lett.*, Vol. 105, 133514, 2014.
27. Li, H. M., S. B. Liu, S. Y. Liu, S. Y. Wang, G. W. Ding, H. Yang, Z. Y. Yu, and H. F. Zhang, "Low-loss metamaterial electromagnetically induced transparency based on electric toroidal dipolar response," *Appl. Phys. Lett.*, Vol. 106, 083511, 2015.
28. Zhu, L., L. Dong, F. Y. Meng, and Q. Wu, "Wide-angle and polarization-independent electromagnetically induced transparency-like effect based on pentacyclic structure," *J. Opt.*, Vol. 16, 015103, 2014.
29. Ren, M., Y. F. Yu, J. M. Tsai, H. Cai, W. M. Zhu, D. L. Kwong, and A. Q. Liu, "Design and experiments of a nano-opto-mechanical switch using EIT-like effects of coupled-ring resonator Solid-State Sensors," *Actuators and Microsystems Conference*, 1436–1439, Beijing, China, 2011.
30. Zhang, J. F., W. Liu, Z. H. Zhu, X. D. Yuan, and S. Q. Qin, "Strong field enhancement and light-matter interactions with all-dielectric metamaterials based on split bar resonators," *Optics Express*, Vol. 22, 30889–30898, 2014.
31. Li, L. Y., J. F. Wang, H. Ma, J. Wang, M. D. Feng, H. L. Du, M. B. Yan, J. Q. Zhang, S. B. Qu, and Z. Xu, "Achieving all-dielectric metamaterial band-pass frequency selective surface via high-permittivity ceramics," *Appl. Phys. Lett.*, Vol. 108, 122902, 2016.
32. Zhao, Q., J. Zhou, F. L. Zhang, and D. Lippens, "Mie resonance-based dielectric metamaterials," *Materials Today*, Vol. 12, 60–69, 2009.
33. Jahani, S. and Z. Jacob, "All-dielectric metamaterials," *Nature Nanotechnology*, Vol. 11, 23–36, 2016.
34. Wei, Z. C., X. P. Li, N. F. Zhong, X. P. Tan, X. M. Zhang, H. Z. Liu, H. Y. Meng, and R. S. Liang, "Analogue electromagnetically induced transparency based on low-loss metamaterial and its application in nanosensor and slow-light device," *Plasmonics*, Vol. 12, 1–7, 2016.
35. Kang, M., Y. N. Li, J. Chen, J. Chen, Q. Bai, H. T. Wang, and P. H. Wu, "Slow light in a simple metamaterial structure constructed by cut and continuous metal strips," *Appl. Phys. B*, Vol. 100, 699–703, 2010.